Dopamine-modified halloysite as new anticancer drug carrier system

Ecem Tansik[1)] (ORCID ID: 0009-0003-1180-2535)**, Hatice Kaplan Can**[1), *)] (0000-0002-2886-0788)

DOI: https://doi.org/10.14314/polimery.2025.5.3

Abstract: A new anticancer drug carrier system based on polydopamine-functionalized halloysite (PDA-HNT) was developed. Hansen solubility parameters were used to select 5-fluorouracil (5-FU) as an anticancer drug. The obtained system was characterized by Fourier transform infrared spectroscopy (FT-IR), X-ray photoelectron spectroscopy (XPS), thermogravimetric analysis (TGA), and nuclear magnetic resonance (^{1}H NMR, ^{19}F-NMR). It was shown that PDA-HNT may be a promising drug nanocarrier for delivery systems in cancer therapy.

Keywords: halloysite, polydopamine, 5-fluorouracil, drug carrier systems, Hansen solubility parameters.

Haloizyt modyfikowany dopaminą jako nowy system dostarczania leków przeciwnowotworowych

Streszczenie: Opracowano nowy system dostarczania leków przeciwnowotworowych oparty na haloizycie funkcjonalizowanym polidopaminą (PDA-HNT). Na podstawie parametr**ów** rozpuszczalności Hansena jako lek przeciwnowotworowy wybrano 5-fluorouracyl (5-FU). Otrzymany system scharakteryzowano za pomocą spektroskopii w podczerwieni z transformacją Fouriera (FT-IR), spektroskopii fotoelektronów rentgenowskich (XPS), analizy termograwimetrycznej (TGA), magnetycznego ^{1}H- rezonansu jądrowego (^{1}H NMR, ^{19}F-NMR). Wykazano, że PDA-HNT może być obiecującym nanonośnikiem w systemach dostarczania leków w terapii nowotworowej.

Słowa kluczowe: haloizyt, polidopamina, 5-fluorouracyl, systemy dostarczania leków, parametry rozpuszczalności Hansena.

Cancer encompasses a group of diseases where atypical cells proliferate excessively and without regulation. These malignant cells can invade and disrupt adjacent tissues, and they can also spread, or metastasize, to other areas of the body through the circulatory and lymphatic systems [1]. According to the World Health Organization's 2022 report, cancer was a leading cause of death globally in 2020, accounting for approximately 10 million deaths. [2]. Cancer treatments are currently performed using methods such as surgery, chemotherapy, radiation therapy, hormone therapy, photodynamic therapy, or immunotherapy [3]. Chemotherapy is a type of cancer treatment that uses one or more cancer-preventing drugs (chemotherapeutic agents) as part of a standard chemotherapy regimen.

There are several polymer-based drug delivery systems formulated to improve the therapeutic outcomes of anticancer drugs. That includes polymeric capsules, polymeric nanoparticles, dendrimers, micelles, hydrogels, nanogels, in situ gels, polymer-drug conjugates, and nanoliposomes [4]. Polymer-drug conjugates have long been a mainstay in the field of drug delivery, following the successful clinical translation of several conjugates. Polymer-drug conjugate systems are pharmacologically active macromolecular structures composed of one or more therapeutic agents covalently attached to a polymeric carrier [5].

Halloysite is a highly economical, naturally abundant, and suitable clay nanomaterial extracted from sediments. The outer diameter is 40–70 nm, the inner diameter 10–20 nm, and the length 500–1500 nm. Due to their larger surface area, positively charged inner surface (Al-OH groups), and negatively charged outer surface, halloysites can effectively bind with various synthetic (such as polymers, drug active agents) and biological components. The presence of siloxane, silanol, and alumina (Al\O) groups on the external surface of halloysite enhances its propensity to bind with various functional groups via Van der Waals forces, hydrogen bonding, electrostatic, and covalent interactions. The porous nature of the halloysite surface enables it to function as both a dopant and a template

[1)] Division of Polymer Chemistry, Department of Chemistry, Faculty of Science, Hacettepe University, 06800 Beytepe Ankara, Türkiye.

[*)] Author for correspondence: hkaplan@hacettepe.edu.tr

for polymers. These pores also facilitate the diffusion of monomers, enabling in situ polymerization. Moreover, halloysite modified environmentally friendly and nontoxic polymers finds widespread application in gene and sustained drug delivery [6–7].

Polydopamine (PDA) is a biomimetic, self-polymerizing polymer that can be readily deposited on a wide variety of materials. In the biomedical field, polydopamine is employed in applications including tissue engineering, biosensing, bioimaging, molecular imprinting, wound dressing, and drug delivery. Owing to its excellent biocompatibility, ease of preparation, unique physicochemical properties, and versatile functionality, polydopamine is most commonly used for drug delivery applications and, additionally, for chemotherapy, targeted therapy and photothermal therapy, as well as combinations such as chemo-thermal therapy, photodynamic-photothermal therapy and chemo-photothermal therapy [8, 9]. Polydopamine is synthesized through the auto-oxidation of dopamine monomers, which can occur via solution oxidation, electro polymerization, or enzymatic oxidation. Among these methods, solution oxidation is the most common technique due to the ease of dopamine's self-polymerization and its feasibility in non-demanding environments or complex systems. The most common and straightforward method for synthesizing PDA involves the air oxidation of dopamine (typically dopamine hydrochloride) in an aqueous alkali solution. Under these conditions, PDA precipitates as a dark black solid over a period of hours (usually 12 hours or more). Dopamine can self-polymerize, and it can also be polymerized onto various substrates such as metals and metal complexes, halloysite, mesoporous structures, graphene oxide and other polymers. Some methods have been reported in the literature for the modification of halloysite surfaces with polydopamine to form nanocomposites [9–14].

Considering these properties, the integration of halloysite and polydopamine presents a promising strategy for enhancing the delivery and efficacy of chemotherapeutic agents. Halloysite's tubular and porous structure makes it suitable for drug delivery applications, providing a stable platform for the loading and transport of therapeutic compounds. Meanwhile, polydopamine contributes to improved biocompatibility, targeted delivery, and multifunctional therapeutic potential through its surface-modifying capabilities.

Therefore, the aim of this study is to investigate the potential of dopamine-modified halloysite nanotubes (PDA-HNT) as an anticancer drug delivery system. Combining the unique structural and functional properties of both materials, this research aims to theoretically and experimentally investigate their conjugation with anticancer drugs, which will contribute to the development of more efficient and targeted cancer therapies.

EXPERIMENTAL PART

Materials

Halloysite nanotubes (HNT) was supplied from Eczacıbaşı Esan Co. Ltd. Istanbul, Turkey; dimethylformamide (DMF), and triethylamine (TEA), dopamine, ammonium chloride coupled with 5-fluorouracil (5-FU) were obtained from Sigma Aldrich St. Louis, USA and ethanol was supplied by Merck KGaA, Darmstadt, Germany.

Preparation of PDA modified HNT

A 2.00 g of HNT was dispersed in 65 mL of deionized water at 500 rpm for 2 h. Subsequently, 2 mL of ammonium chloride and 40 mL of ethanol were simultaneously added. The resulting solution was stirred at 30°C and 200 rpm for 30 min. Solution pH was adjusted to approximately 8.5. Separately, 0.50 g of dopamine was dissolved in 10 mL of deionized water and added to the HNT-buffer system. The process was carried out at 250 rpm for 24 h. PDA-HNT was dried at room temperature.

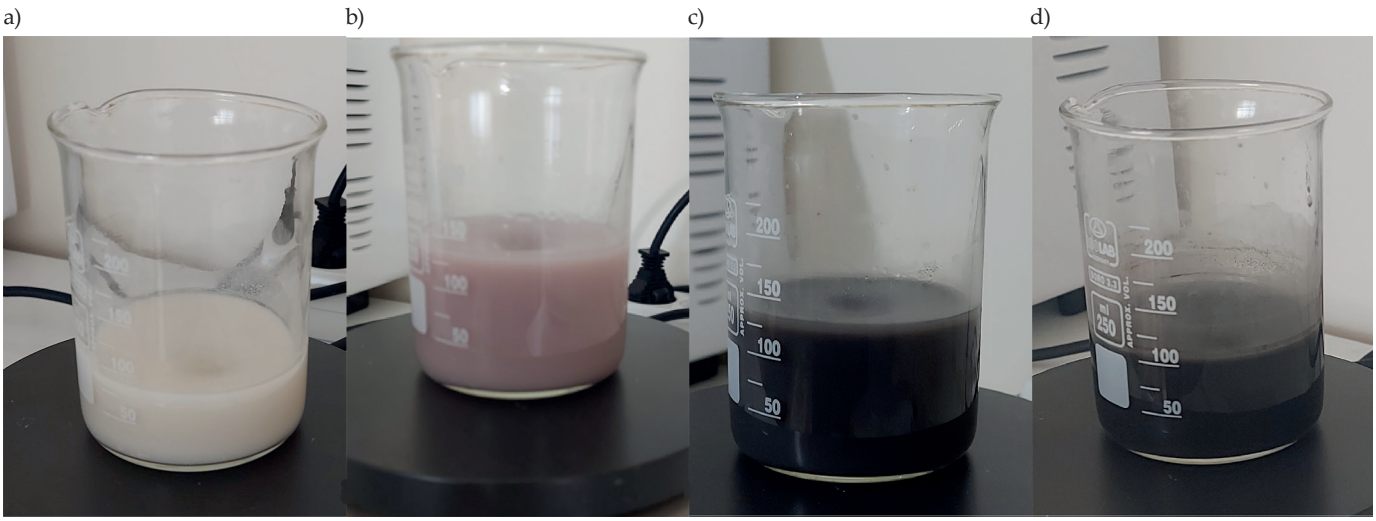

Fig. 1. PDA-HNT polymerization process: a) beginning, b) 3 h, c) 24 h, d) end (product precipitation)

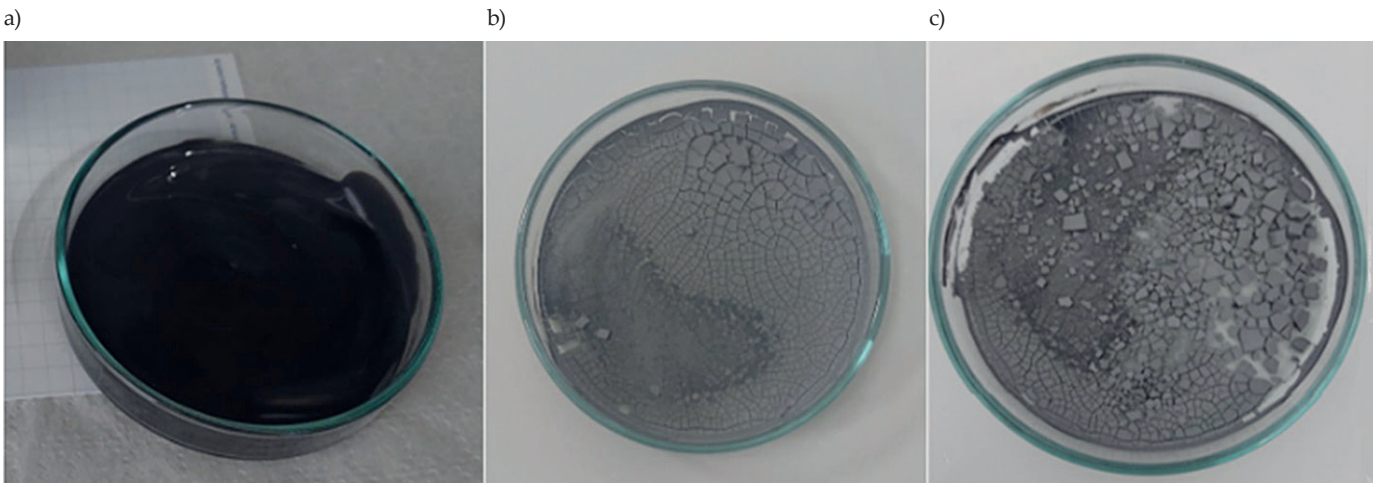

Fig. 2. Product after polymerization and drying process: a) PDA-HNT complex separated from the solvent, b) 7 days of drying, c) 14 days of drying

Preparation of modified PDA-HNT with 5-fluorouracil system

0.35 g of 5-FU and 0.25 g of TEA were stirred in 25 mL of DMF at 70 °C for 1 h. Then the solution was cooled in an ice bath. In parallel, 0.70 g of PDA-HNT was dispersed in 10 mL of DMF at room temperature for 30 min and next stirred at room temperature for 2 h. The resulting PDA-HNT and 5-fluorouraacil system (PDA-HNT/5-FU) was precipitated, separated from the solvent, and dried in the open air.

Methods

Calculations were performed using the Hansen solubility parameters in practice (HSPiP) software. The functional groups of samples were analyzed by Fourier transform infrared spectroscopy, FT-IR (Shimadzu IR-Xross, Kyoto, Japan) using an ATR attachment. Twenty scans were collected at a resolution of 4 cm^{-1}. The changes in the chemical structure on the surface were obtained by X-ray photoelectron spectroscopy (XPS) spectrometer (Physical Electronics, PHI 5000 VersaProbe Chanhassen, USA). The ^{1}H NMR and ^{19}F-NMR techniques were performed using NMR spectrometer (Bruker 400 MHz AV, Billerica USA, and Bruker Ultrashield TM 300 MHz NMR spectrometer Billerica USA in that order). Samples dissolved in DMSO-*d6*. Thermogravimetric analysis (TGA) was performed using a thermogravimetric analyzer (TA Instruments Q600 SDT, New Castle, USA) under nitrogen atmosphere between 25°C and 800°C at heating rate of 20°C/min.

RESULTS AND DISCUSSION

Solubility and solubility parameters calculations

The production of chemicals such as pharmaceuticals, coatings, cosmetics, paints, and food products often involves multicomponent mixtures. Today, there is a pressing need for reliable methods to predict the fundamental physicochemical properties of materials, especially their solubility, miscibility with other chemicals, and interactions with the environment to meet process and product quality specifications. A simpler and more commonly used approach is the calculation of solubility parameters [15].

Solubility parameters are employed in a wide range of fields, particularly in the coating and paint industry. Some examples include the selection of suitable solvent systems for polymers [16], the prediction and understanding of drug distribution in microspheres using the solubility parameter [17], the prediction of cocrystal structures [18], the creation of self-assembling gel systems [19], and the prediction of optimal polymer and solvent selection for molecularly imprinted polymeric systems to achieve ideal drug carrier [20].

In 1916, Hildebrand proposed a correlation between solubility and the internal pressure of a solvent. Scatchard introduced the concept of 'cohesive energy density' into Hildebrand's equation in 1931, and in 1949, Hildebrand defined a solubility parameter, which is the square root of the cohesive energy density. For nonpolar solvents, the solubility parameter, δ is equal to the square root of the molar evaporation energy, as shown in the Equation 1 [21]:

$$\delta = \sqrt{\frac{\Delta E_v}{V}} \tag{1}$$

where: V is the molar volume and ΔE_v is the molar internal energy of vaporization. The molar internal energy of vaporization can be defined as Equation 2:

$$\Delta E_v = \Delta H_v - RT \tag{2}$$

where: ΔH_v is the molar enthalpy of vaporization, T is the temperature, and R is the ideal gas constant. The original and commonly used unit for the solubility parameter is $(cal/cm^3)^{(1/2)}$. In the SI system, it is $MPa^{(1/2)}$.

For a dissolution process to be thermodynamically favorable, the Gibbs free energy change, ΔG_m, must be negative, as described in the Equation 3:

$$\Delta G_m = \Delta H_m - \Delta S_m \quad (3)$$

where: ΔH_m is the enthalpy change, ΔS_m is the entropy change, and T is the temperature in Kelvin. ΔS_m is positive, and the sign of ΔH_m determines whether the process is spontaneous.

Due to its simplicity, Hildebrand's single solubility parameter has been extensively employed in both academic and industrial contexts for an extended period. Nonetheless, this parameter was solely applicable to apolar solvents, excluding significant factors such as hydrogen bonding and dipole-dipole interactions in the calculations [22].

In 1967, Hansen proposed that the cohesive forces binding liquids, comprising nonpolar interactions, hydrogen bonds, and dipole-dipole interactions, are disrupted during vaporization. He further suggested that these factors should be incorporated into the calculation of vaporization energy. Consequently, he subdivided Hildebrand solubility parameters into three components: atomic dispersion force (δ_D), molecular dipole-dipole interactions (δ_P), and hydrogen bonding (δ_H) interactions. Collectively, δ_D, δ_P, and δ_H are termed Hansen Solubility Parameters, and the overall solubility parameter (δ_T) can be expressed as Equation 4:

$$(\delta_T)^2 = (\delta_D)^2 + (\delta_P)^2 + (\delta_H)^2 \quad (4)$$

In his formulation of Hansen parameters, Hansen determined the hydrogen bonding parameter (δ_H) by subtracting the dispersion (δ_D) and polarizability (δ_P) components from the total parameter (δ_T). Alternatively, the group contribution method, as developed by van Krevelen, Hoy, and Hoftijzer provides an avenue for computing the hydrogen bonding parameter.

Departing from the Hildebrand single-component parameter, Hansen eschewed treating all molecular interactions as a holistic measure of cohesion and comparing the compatibility of energy densities. Instead, he introduced a coordinate system centered on the solute of interest within a three-dimensional interaction field [23]. The intermolecular distance between the solvent and solute is denoted as R_a and is computed using Equation 5:

$$R_a = \sqrt{4(\delta_{D2} - \delta_{D1})^2 - (\delta_{P2} - \delta_{P1})^2 - (\delta_{H2} - \delta_{H1})^2} \quad (5)$$

Furthermore, Hansen introduced the concept of relative energy difference (RED). RED is calculated as the ratio of R_a to the Hansen radius, R_o. The Hansen radius, R_o, signifies the maximal attainable R_a value at solvation-permissive sites, described in Equation 6:

$$\text{RED} = \frac{R_a}{R_o} \quad (6)$$

A RED value of zero signifies that the system is in a state of minimum energy, with no driving force for further interaction. As the RED value deviates from zero, it quantifies the degree of mismatch between the solvent and solute, resulting in an increasing energy difference.

In this study, calculations were performed using the Hansen solubility parameters in practice (HSPiP) software (version 5.3.06). Developed by Abbott, Hansen, and Yamamoto, HSPiP is a comprehensive computational tool that models molecular interactions based on Hansen's three-dimensional solubility parameters. HSPiP facilitates the creation of three-dimensional (δ_P-δ_H-δ_D) diagrams, enabling the identification of suitable solvents for various substances and the visualization of molecular interactions. Furthermore, to address the challenges associated with interpreting three-dimensional diagrams, two-dimensional projections (δ_P-δ_H, δ_P-δ_D, δ_H-δ_D) can be generated [24]. The solubility parameters of dopamine and polydopamine, along with selected anticancer drugs, are summarized in Table 1 and Table 2. And their 3D graphics are shown in Figure 3.

Based on theoretical relative energy difference (RED) values, doxorubicin exhibited the lowest RED value when compared with dopamine (2.53), followed closely by 5-fluorouracil (2.76), as shown in Table 2. Upon theoreti-

T a b l e 1. Solubility parameters of dopamine and some antineoplastics

Compound	δ_D	δ_P	δ_H	δ_T	RED
Dopamine	19.6	7.6	15.2	25.9	–
Doxorubicin	20.8	13.6	7.4	25.9	2.53
5-florourasil	18.8	18.4	13.6	29.6	2.76
Hydroxyurea	20.7	16.4	32.1	41.6	4.80

T a b l e 2. Solubility parameters of PDA and selected anticancer drugs

Compound	δ_D	δ_P	δ_H	δ_T	RED
PDA	21.1	6.3	12.4	25.3	–
Doxorubicin	20.8	13.6	7.4	25.9	2.22
5-florourasil	18.8	18.4	13.6	29.6	3.25
Hydroxyurea	20.7	16.4	32.1	41.6	4.80

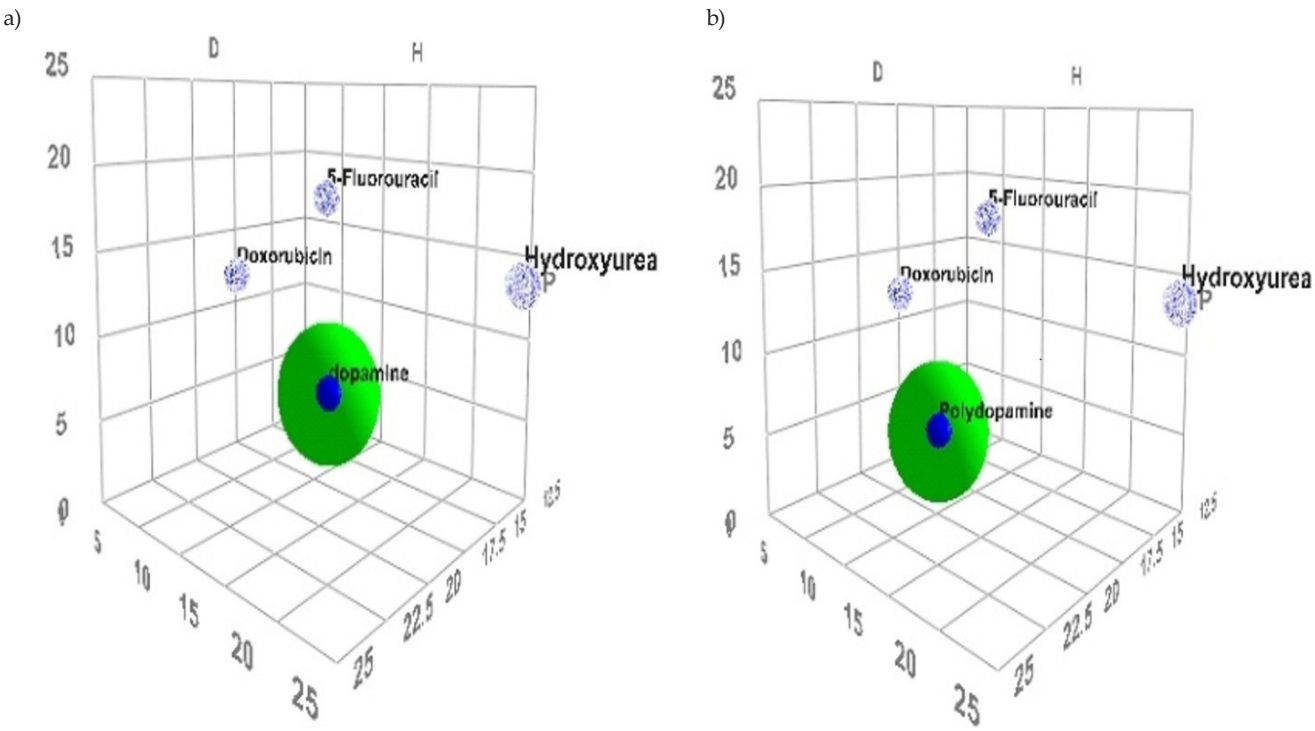

Fig. 3. 3-D diagrams of: a) dopamine and anticancer drugs, b) PDA and anticancer drugs

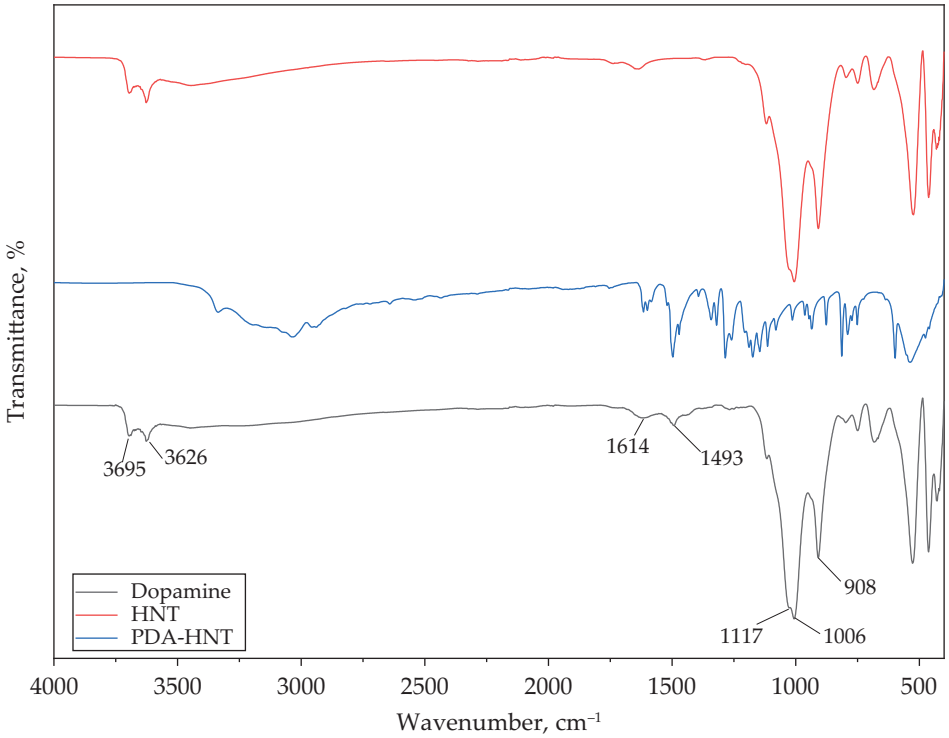

Fig. 4. FT-IR spectra of dopamine, HNT and PDA-HNT

cal polymerization of dopamine into PDA (Table 3), RED values changed due to the altered solubility characteristics of the polymer, although the relative ranking of the anticancer drugs remained consistent.

Although doxorubicin exhibited slightly better theoretical affinity for both dopamine and PDA matrices, 5-fluorouracil was selected for coupling due to several practical considerations. Its smaller molecular size is advantageous for diffusion through the porous PDA-HNT network, while its moderate interaction with the polymer matrix, as reflected by the RED value, suggests a more favorable release profile. Furthermore, 5-fluoro-

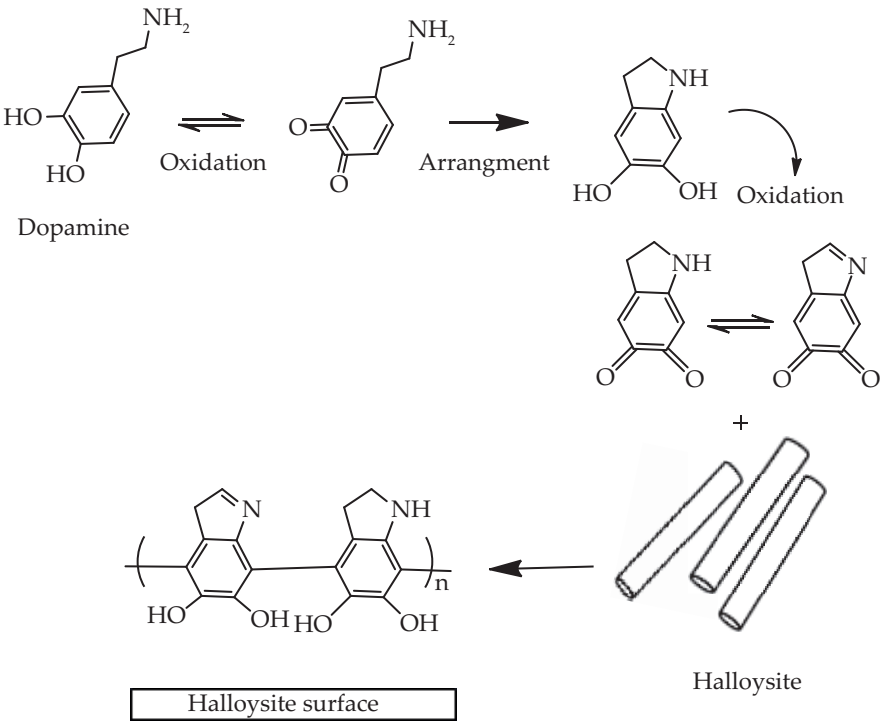

Scheme 1. Dopamine oxidation polymerization on HNT surface

uracil displays sufficient chemical stability to remain intact during the conjugation process. Taken together, these factors support the choice of 5-fluorouracil as a suitable model drug for the development of PDA-based nanocomplex [29–30].

Characterization of PDA-HNT complex

FT-IR analysis

PDA was coated on the surfaces of HNT through self-polymerization of dopamine in HNTs dispersion. Figure 4 presents comparative FT-IR spectra of HNT, dopamine, and PDA-HNT. The dopamine is oxidized and polymerized into PDA, and a crosslinked polymer structure is formed (Scheme 1). Polymerization occurs in alkaline conditions with the presence of oxygen.

FT-IR spectrum of PDA-HNT exhibited characteristic peaks corresponding to -OH stretching vibrations of HNT at 3695 and 3626 cm^{-1}, Al-OH stretching vibrations at 908 cm^{-1}, and Si-O stretching vibrations in the region of 1006–1117 cm^{-1}. The presence of dopamine in the structure was confirmed by -NH bending vibration at 1614 cm^{-1} and C=C bending vibration at 1493 cm^{-1} [31–32].

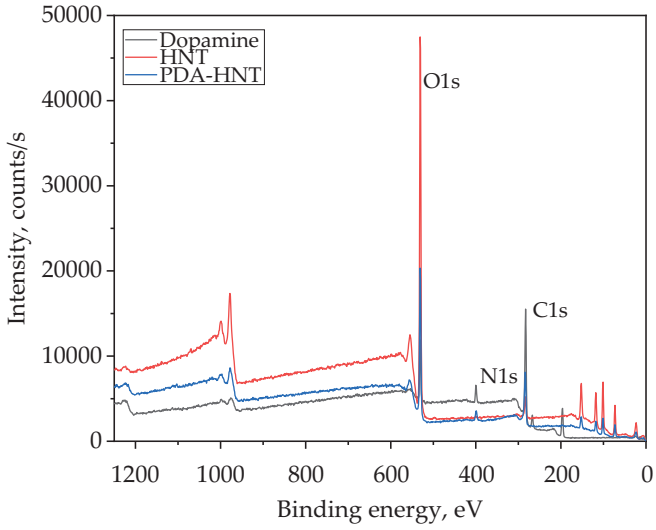

Fig. 5. XPS spectra of HNT, dopamine and PDA-HNT (1200-0 eV)

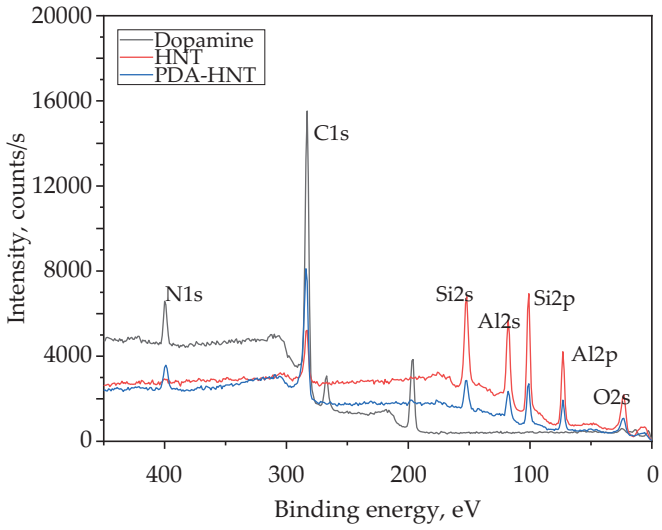

Fig. 6. XPS spectra of HNT, dopamine and PDA-HNT (450-0 eV)

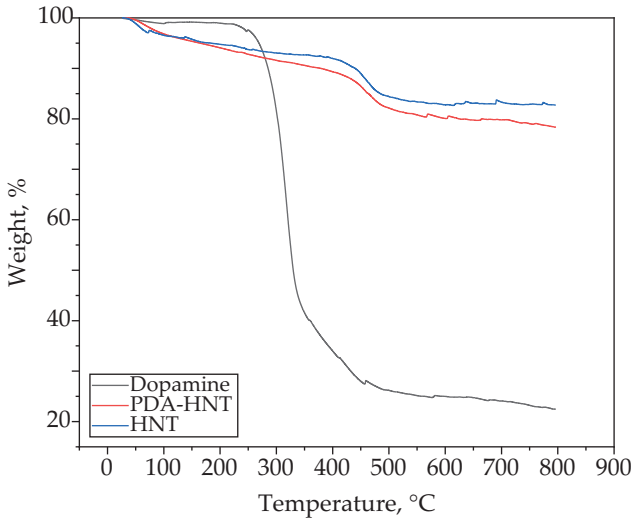

Fig. 7. TGA thermograms of HNT, dopamine and PDA-HNT

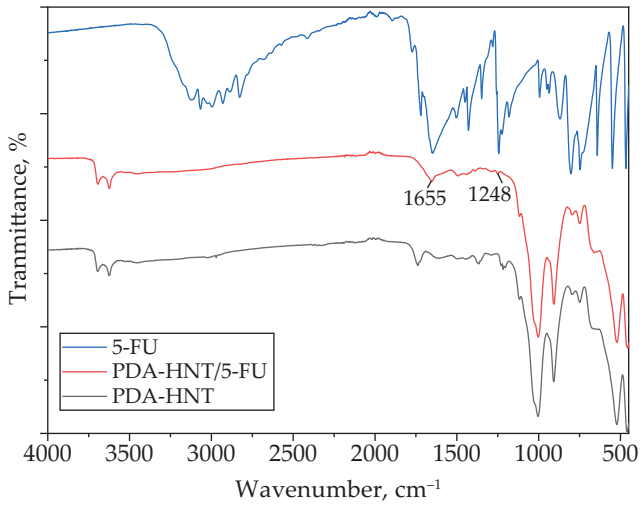

Fig. 8. FT-IR spectra of 5-FU, PDA-HNT/5-FU and PDA-HNT

X-ray photoelectron spectroscopy analysis

X-Ray photoelectron spectroscopy (XPS) can be applied to a broad range of materials and provides valuable quantitative and chemical state information from the surface of the material being studied. Analysis of XPS spectra revealed the presence of characteristic Al2p, Si2p, Al2s, and Si2s peaks in both HNT and PDA-HNT within the binding energy range of 60-170 eV, indicating the existence of HNT in the structure of PDA-HNT (Figure 5 and 6).

A distinct N1s peak, corresponding to the nitrogen element present in dopamine but absent in pure HNT, was observed at approximately 400 eV in the PDA-HNT structure. Additionally, the intensity of the C1s peak at 283 eV was significantly higher in PDA-HNT compared to pure HNT. These two observations provide evidence for the occurrence of dopamine polymerization on the HNT surface. It was found that the carbon content (C1s) increased from 9.6% in HNT to 40.6% in PDA-HNT, while nitrogen, absent in pure HNT, was observed at a level of 4.6% in PDA-HNT.

The XPS spectrum shows that the peak of nitrogen of PDA/HNT becomes stronger than that of HNTs and the peak of Si of PDA-HNT is weaker than that of HNT. This phenomenon suggests that the elements content of the two samples change significantly and reveals that PDA wrapped on the surface of HNTs successfully.

Thermogravimetric analysis

TGA is a kind of useful method for investigating differences in physical/chemical properties of materials. TGA implemented as a function of weight loss at a regular increasing temperature under constant heating rate/or time. As can be seen from the thermogram it is revealed that dopamine experienced a 70% mass loss between 225°C and 425°C (Figure 7). Upon reaching approximately 800°C, the mass loss of dopamine reached approximately 78%. The thermogram of HNT showed a mass loss of approximately 8% up to 400°C, followed by a 10% mass loss between 400°C and 480°C. At 800°C, the mass loss did not exceed 20%. PDA-HNT exhibited mass loss behavior like HNT, but due to the presence of dopamine in its structure, the mass loss reached approximately 22% at 800°C.

Characterization of PDA-HNT and 5–fluorouracil drug delivery system

Halloysites are ideal candidates for bionanocomposite materials, since the alumina and silica groups on the HNT surface and at the ends of the tubes facilitate hydrogen bonding with biological components. HNTs are being used as nanoreservoirs and nanocarriers for the carrier of drugs by adsorption, intercalation, and tubular entrapment methods for loading medicines into the lumen as well as on the surface of HNT.

FT-IR analysis

The comparative FT-IR spectra presented in Figure 8 reveals PDA-HNT/5-FU structure. The characteristic -C=O stretching vibration of 5-FU at approximately 1655 cm^{-1} and C-N stretching vibration of PDA-HNT/5-FU at 1248 cm^{-1} were both observed in PDA-HNT/5-FU spectrum [25–26].

^{1}H NMR analysis of drug delivery system

^{1}H NMR analysis (as shown in Figure 9) of PDA-HNT/5-FU revealed peaks characteristic of 5-FU at approximately 7.8 ppm (A, B), 10.7 ppm (C), and 11.5 ppm (B). These peaks were also observed in NMR spectra of 5-FU itself, confirming the presence of 5-FU within the PDA-HNT/5-FU structure. Moreover, the peaks corresponding to the CH_2-C and CH_2-N structures of PDA,

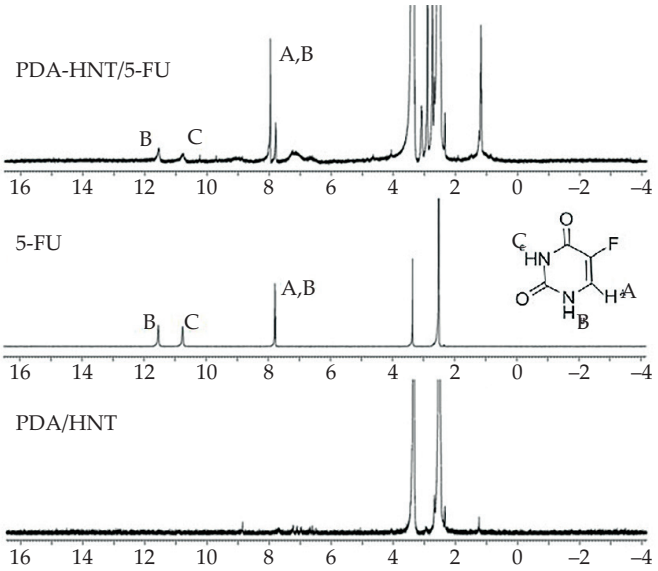

Fig. 9. ^{1}H NMR spectra of PDA-HNT/5-FU, 5-FU, and PDA-HNT

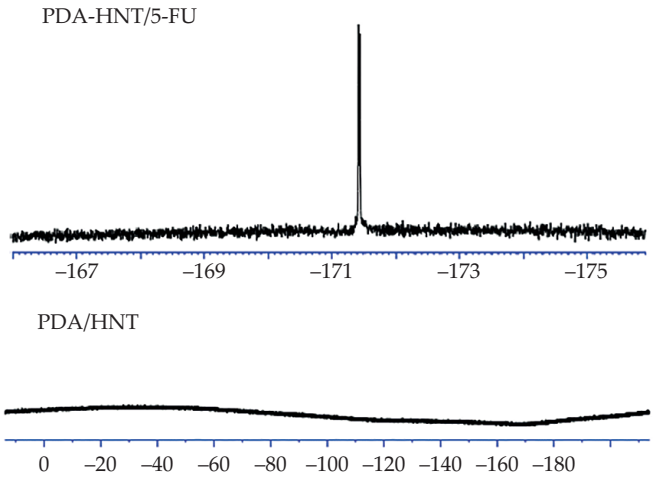

Fig. 10. ^{19}F NMR spectra of PDA-HNT/5-FU and PDA-HNT

observed at 1.4 ppm and 2.9 ppm in PDA-HNT, were likewise detected in the PDA-HNT/5-FU sample, indicating the successful coupling of PDA to 5-FU [27–28].

^{19}F NMR analysis of drug delivery systems

^{19}F NMR (as shown in Figure 10) spectroscopy was employed to elucidate the structural differences between PDA-HNT and PDA-HNT/5-FU. The absence of a fluorine peak in the PDA-HNT spectrum, in contrast to the presence of a fluorine peak at -171.4 ppm attributed to 5-FU in PDA-HNT/5-FU spectrum, indicated the successful coupling of 5-FU to PDA-HNT/5-FU structure.

CONCLUSIONS

Halloysite was functionalized with PDA and then coupled with an anticancer drug (5-fluorouracil) selected based on Hansen solubility parameters. FT-IR, XPS, TGA, ^{1}H NMR and ^{19}F NMR studies confirmed the successful coupling of 5-FU with PDA-HNT. Due to its biocompatibility and low cytotoxicity, PDA-HNT has great potential as a nanocarrier of active substances in controlled drug delivery systems, especially in cancer therapy.

Authors contribution

E.T.: methodology, formal analysis, investigation, writing-original draft; H.K.C: conceptualization, methodology, formal analysis, investigation, visualization, writing-review and editing, investigation, editing. All authors have read and agreed to the published version of the manuscript.

Funding

This research received no external funding.

Conflict of interest

The authors declare no conflict of interest.

REFERENCES

[1] Brown J.S., Amend S.R., Austin R.H. *et al.: Molecular Cancer Research* **2023,** *21*, 1142. https://doi.org/10.1158/1541-7786.MCR-23-0411

[2] Ferlay J., Colombet M., Soerjomataram I. *et al.: International Journal of Cancer* **2021**, *149*, 778. https://doi.org/10.1002/ijc.33588

[3] Sylvestre, B: *Dalton Transactions* **2018**, *47*, 10330. https://doi.org/10.1039/C8DT01585F

[4] Alven S., Nqoro X., Buyana B. *et al*: *Pharmaceutics* **2020**, *12*, 406. https://doi.org/10.3390/pharmaceutics12050406

[5] Ekladious I., Colson Y.L., Grinstaff M.W.: *Nature Reviews Drug Discovery* **2019**, *18*, 273. https://doi.org/10.1038/s41573-018-0005-0

[6] Pramanik A., Sciortino A., Reale M. *et al.: ACS Applied Nano Materials* **2023**, *6*, 15896. https://doi.org/10.1021/acsanm.3c02840

[7] Satish S., Tharmavaram M., Rawtani D.: *Nanobiomedicine* **2019**, *6*, 1. https://doi.org/10.1177/1849543519863625

[8] Hemmatpour H.: Functionalization of Halloysite Nanotubes for Environmental and Drug Delivery Applications. University of Groningen, Groningen **2022**, p. 202. https://doi.org/10.33612/diss.204280083
[9] Ambekar R.S., Kandasubramanian B.: *Biomaterials Science* **2019**, *7*, 1776. https://doi.org/10.1039/C8BM01642A
[10] Mousavi S.M., Zarei M., Hashemi S.A.R.: *Medicinal Chemistry* **2018,** *8,* 218. https://doi.org/10.4172/2161-0444.1000516
[11] Liebscher J.: *European Journal of Organic Chemistry* **2019**, *2019* 4976. https://doi.org/10.1002/ejoc.201900445
[12] Yanlan L., Kelong A., Lehui L.: *Chemical Reviews* **2014**, 114, 5057. https://doi.org/10.1021/cr400407a
[13] Wu F., Zheng J., Li Z. *et al.: Chemical Engineering Journal* **2019**, *359*, 672. https://doi.org/10.1016/j.cej.2018.11.145
[14] Ganguly S., Das T.K., Mondala S. *et al.: RSC Advances* **2016**, *6*, 105350. https://doi.org/10.1039/C6RA24153K
[15] Stefanis E., Panayiotou C.: *International Journal of Pharmaceutics* **2012**, 426, 29. https://doi.org/10.1016/j.ijpharm.2012.01.001
[16] Güner, A.: *European Polymer Journal* **2004**, *40*, 1587. https://doi.org/10.1016/j.eurpolymj.2003.10.030
[17] Vay K., Scheler S., Friess W.: *International Journal of Pharmaceutics* **2011,** *416*, 202. https://doi.org/10.1016/j.ijpharm.2011.06.047
[18] Mohammad M.A., Alhalaweh A., Velaga S.P.: *International Journal of Pharmaceutics* **2011**, *407*, 63. https://doi.org/10.1016/j.ijpharm.2011.01.030
[19] Bonnet J., Suissa G., Raynalab M. *et al.: Soft Matter* **2015**, *11*, 2308. https://doi.org/10.1039/C5SM00017C
[20] Madsen C.G., Skov A., Baldursdottir S. *et al.: European Journal of Pharmaceutics and Biopharmaceutics* **2015**, *92*, 1. https://doi.org/10.1016/j.ejpb.2015.02.001
[21] Van Krevelen, D.W., Te Nijenhuis K., ''Properties of Polymers: Their Correlation with Chemical Structure; their Numerical Estimation and Prediction from Additive Group Contributions'', Elsevier, Amsterdam, The Netherlands, 2009, p. 189–190.
[22] Hansen C.M.: *Progress in Organic Coatings* **2004**, *51*, 77. https://doi.org/10.1016/j.porgcoat.2004.05.004
[23] Süß S., Sobisch T., Peukert W. *et al.: Advanced Powder Technology* **2018**, *29*, 1550. https://doi.org/10.1016/j.apt.2018.03.018
[24] Abbott S., Hansen C.M., Yamamoto H.: Hansen Solubility Parameters in Practice – Complete with software, data, and examples. E-book. 5th ed. 2015.
[25] Samy, M., Abdallah, H.M., Awad, H.M. *et al.: Polymer Bulletin* **2023**, *80*, 6197. https://doi.org/10.1007/s00289-022-04308-w
[26] Singh G., Faruk A., Bedi P.M.S.: *Journal of Drug Delivery and Therapeutics* **2018**, *8*, 111. https://doi.org/10.22270/jddt.v8i6.2030
[27] Liebscher J., Mrówczyński R., Scheidt H.A. *et al.*: *Langmuir* **2013**, *29*, 10539. https://doi.org/10.1021/la4020288
[28] Gan, B.K., Rullah, K., Yong, C.Y. *et al.*: *Scientific Reports* **2020**, *10*. https://doi.org/10.1038/s41598-020-73967-4
[29] Rochard E.B., Barthès D.M., Courtois P.Y: *American Journal of Health-System Pharmacy* **1992,** *49*, 619. http://doi.org/10.1093/ajhp/49.3.619
[30] Singh M.B., Vishvakarma V.K., Lal A.A. *et. al.: Journal of the Indian Chemical Society* **2022**, *99*, 100790. https://doi.org/10.1016/j.jics.2022.100790
[31] Ghorbani F., Ali Z. and Sahranavard M.: *Biomedical Engineering/Biomedizinische Technik* **2020**, 65, 273. https://doi.org/10.1515/bmt-2019-0061
[32] Cao X., Liu X. H., Yang X. *et. al.*: *Composites Science and Technology*, **2020**, 191, 108071. https://doi.org/10.1016/j.compscitech.2020.108071

Received 20 III 2025.
Accepted 10 IV 2025.